First Order Premelting Transition of Vortex Lattices

Hervé M. Carruzzo and Clare C. Yu

Department of Physics and Astronomy, University of California, Irvine, Irvine, California 92697
(February 1, 2008)

Vortex lattices in the high temperature superconductors undergo a first order phase transition which has thus far been regarded as melting from a solid to a liquid. We point out an alternative possibility of a two step process in which there is a first order transition from an ordinary vortex lattice to a soft vortex solid followed by another first order melting transition from the soft vortex solid to a vortex liquid. We focus on the first step. This premelting transition is induced by vacancy and interstitial vortex lines. We obtain good agreement with the experimental transition temperature versus field, latent heat, and magnetization jumps for YBCO and BSCCO.

Phase transitions involving vortex lattices in the high temperature superconductors is an area of active study [1,2]. Below a critical value of the magnetic field, vortex lattices in YBa$_2$Cu$_3$O$_{7-\delta}$ (YBCO) [3–6] and Bi$_2$Sr$_2$CaCu$_2$O$_8$ (BSCCO) [7–9] undergo a first order phase transition. This conclusion comes from latent heat measurements [6] as well as jumps in the resistivity [3,8,9] and in the magnetization [4,5,7]. It has generally been assumed that this is a melting transition from a vortex solid to a vortex liquid. In this paper we suggest the possibility that the melting transition actually occurs in two steps as the temperature increases; the first step is a first order premelting transition from an ordinary vortex lattice to a soft solid with a small but finite shear modulus, and the second step is the first order melting of the soft solid into a vortex liquid. In this paper we focus on the first step. We present an analytic theory of a first order premelting transition in which the shear modulus jumps discontinuously. The transition is induced by interstitial and vacancy line defects in the vortex lattice which soften the shear modulus c_{66}. We find good agreement with the experimental curve of transition temperature versus field, latent heat and magnetization jumps for YBCO and BSCCO. In the soft solid phase the superconducting phase coherence along the field is destroyed by the wandering of the defect lines which become entangled in the vortices of the soft solid lattice [10,11]. However, since wandering is energetically costly, the superconducting correlation length along the c–axis is long. Finally we speculate about the relation between our proposed two-step transition and the well known peak effect [12,13].

Let us describe our scenario for premelting. Our approach follows that of Granato who showed that interstitial atoms soften the shear modulus of ordinary crystals and lead to a first order transition [14]. We start with a vortex lattice in a clean layered superconductor with a magnetic field H applied perpendicular to the layers along the c-axis. We consider the vortices to be correlated stacks of pancake vortices. We will assume that the transition is induced by topological defect lines, i.e., vacancies and interstitials. In a Delaunay triangulation [15] a vacancy or an interstitial in a triangular lattice is topologically equivalent to a pair of bound dislocations [16] as well as to a twisted bond defect [17]. High temperature decoration experiments [17] and Monte Carlo simulations [16] have found such defects to be thermally excited. The introduction of these defects softens the elastic moduli. Since the energy to introduce interstitials and vacancies is proportional to the elastic moduli, softening makes it easier to introduce more defects. The softening also increases the vibrational entropy of the vortex lattice which leads to a premelting transition. The transition is driven by the increased vibrational entropy of the vortex lines of the lattice, and not by the entropy of the wandering of the defect lines. In fact Frey, Nelson and Fisher [10] showed that a phase transition driven by the entropy of wandering flux lines occurs at a much higher magnetic field than what is observed experimentally. In the vicinity of the experimentally observed first order phase transition, wandering in the transverse direction by more than a lattice spacing is energetically quite costly and therefore rare. (The energy scale is set by $\epsilon_o s$ [1,2]. Here s is the interplane spacing and ϵ_o, the energy per unit length of a vortex, is given by $\epsilon_o = (\phi_o/4\pi\lambda_{ab})^2$ where ϕ_o is the flux quantum and λ_{ab} is the penetration depth for currents in the ab plane.)

Experimentally the resistivity jumps up at the transition from zero to a finite value as the temperature increases. This is consistent with our model since the soft solid will have a finite resistivity due to the motion of interstitial (and vacancy) lines. The barrier for the motion of interstitials is very small [10] and is of order $10^{-3}E_o$ per unit length, where $E_o = 2\epsilon_o$. The defect lines act like a liquid of lines existing in a soft solid host. Notice that if one tries to measure the shear modulus of such a system using resistivity measurements, only the defect lines would move relative to the pinned soft solid and one would deduce the shear modulus was zero [18,19,12].

The first order transition is nucleated in a small re-

gion by a local rearrangement of existing line segments. Slightly above the premelting temperature T_p a vortex line can distort and make an interstitial and a vacancy line segment that locally create a soft solid. This is the analog of a liquid droplet which nucleates melting of a crystal. The role of the surface tension is played by the energy to connect the interstitial segment to the rest of the vortex line. This connection can be a Josephson vortex lying between planes or a series of small pancake vortex displacements spread over several layers. When the length ℓ of the interstitial and vacancy segments equals the critical length ℓ_c, the energy gained by premelting equals the energy cost of the connections. When $\ell > \ell_c$, it is energetically favorable for the defect segments grow to the length of the system.

To study premelting we assume that we have a vortex lattice with interstitial and vacancy lines extending the length of the lattice. Our goal is to find the free energy density as a function of the concentration n of defect lines. The free energy density is $f = f_o + f_w + f_{vib} + f_{wan}$ where f_o is the free energy density of a perfect lattice, f_w is the work needed to introduce a straight interstitial or vacancy line into the lattice, f_{vib} is the vibrational free energy density of the system, and f_{wan} is the free energy due to the wandering of the defect lines over distances large compared to the lattice spacing. We now examine these terms in detail.

f_o, the free energy density of a perfect rigid flux lattice, is given by the London term [10,20]:

$$f_o = \frac{B^2}{8\pi} + \frac{B\phi_o}{32\pi^2\lambda_{ab}^2}\ln\left(\frac{\eta\phi_o}{2\pi\xi_{ab}^2 B}\right), \quad \frac{\phi_o}{4\pi\lambda_{ab}^2} \ll B \ll H_{c2} \tag{1}$$

where B is the spatially averaged magnetic induction, ξ_{ab} is the coherence length in the ab plane, and η is 0.130519 for a hexagonal lattice and 0.133311 for a square lattice [10]. For B near H_{c2}, f_o is given by the Abrikosov free energy [21]

$$f_o = \frac{B^2}{8\pi} - \frac{(H_{c2} - B)^2}{8\pi[1 + (2\kappa^2 - 1)\beta_A]} \tag{2}$$

where the Ginzburg-Landau parameter $\kappa = \lambda_{ab}/\xi_{ab}$, and the Abrikosov parameter β_A is 1.16 for a triangular lattice and 1.18 for a square lattice.

To calculate f_{vib}, we follow Bulaevskii et al. [22]. We denote the displacement of the νth vortex pancake in the nth plane from its equilibrium position by $\mathbf{u}(n, \mathbf{r}_\nu)$ where $\mathbf{u} = (u_x, u_y)$ and the pancake position $\mathbf{r} = (r_x, r_y)$. The Fourier transform $\mathbf{u}(\mathbf{k}, q) = \sum_{n\nu} \mathbf{u}(n, \mathbf{r}_\nu)\exp[\mathbf{i}(\mathbf{k}\cdot\mathbf{r}_\nu + \mathbf{qn})]$. $\mathbf{k} = (\mathbf{k_x}, \mathbf{k_y})$ and q is the wavevector along the c-axis. $f_{vib} = -(k_B T/V)\ln Z_{vib}$ where V is the volume and the vibrational partition function Z_{vib} is given by

$$\ln Z_{vib} = \sum_{\mathbf{k},\mathbf{q}>\mathbf{0},\mathbf{i}} \ln \int \frac{du_R(i\mathbf{k}q)du_I(i\mathbf{k}q)}{\pi\xi_{ab}^2}e^{-\mathcal{F}_{el}/k_B T} \tag{3}$$

where we have divided by the area $\pi\xi_{ab}^2$ of the normal core of a pancake [22]. u_R and u_I are the real and imaginary parts of $\mathbf{u}(\mathbf{k}, \mathbf{q})$ and $i\epsilon\{x, y\}$. The elastic free energy functional associated with these distortions is

$$\mathcal{F}_{el} = \frac{1}{2}v_o \sum_{\mathbf{k}q}\sum_{ij} u_i(q, \mathbf{k})a_{ij}u_j^*(q, \mathbf{k}) \tag{4}$$

where i and $j\epsilon\{x, y\}$, the volume per pancake vortex is $v_o = s\phi_o/B$, and s is the interplane spacing. The $\mathbf{k}$ sum is over a circular Brillouin zone $K_o^2 = 4\pi B/\phi_o$. The matrix a_{ij} is given by $a_{ij} = c_B k_i k_j + (c_{66}k^2 + c_{44}Q^2)\delta_{ij}$ where c_B, c_{66}, and c_{44} are the bulk, shear, and tilt moduli, respectively. $c_B = c_{11} - c_{66}$ for a hexagonal lattice. $Q^2 = 2(1 - \cos qs)/s^2$. Diagonalizing a_{ij} leads to 2 eigenvalues: $A_\ell(kq) = c_{11}k^2 + c_{44}Q^2$ and $A_t = c_{66}k^2 + c_{44}Q^2$, where A is the diagonal matrix, the subscript ℓ denotes longitudinal and t denotes transverse. Using this, we can integrate over u in (3); the remaining sums over $\mathbf{k}$ and q are done numerically. At low fields ($b = B/H_{c2} < 0.25$), the elastic moduli are given by [1,2]

$$c_{66} = \frac{B\phi_o\zeta}{(8\pi\lambda_{ab})^2}$$
$$c_{11} = \frac{B^2[1 + \lambda_c^2(k^2 + Q^2)]}{4\pi[1 + \lambda_{ab}^2(k^2 + Q^2)](1 + \lambda_c^2 k^2 + \lambda_{ab}^2 Q^2)}$$
$$c_{44} = \frac{B^2}{4\pi(1 + \lambda_c^2 k^2 + \lambda_{ab}^2 Q^2)} + \frac{B\phi_o}{32\pi^2\lambda_c^2} \tag{5}$$
$$\times \ln\frac{\xi_{ab}^{-2}}{K_o^2 + (Q/\gamma)^2 + \lambda_c^{-2}} + \frac{B\phi_o}{32\pi^2\lambda_{ab}^4 Q^2}\ln(1 + \frac{Q^2}{K_o^2})$$

where λ_c is the penetration depth for currents along the c-axis, $\gamma = \lambda_c/\lambda_{ab}$ is the anisotropy, and $\zeta = 1$. At high fields ($b > 0.5$) [1,2], c_{66} is altered by the factor $\zeta \approx (1 - 0.5\kappa^{-2})(1 - b)^2(1 - 0.58b + 0.29b^2)$ and the penetration depths in c_{11} and c_{44} are replaced by $\tilde{\lambda}^2 = \lambda^2/(1 - b)$ where λ denotes either λ_{ab} or λ_c. In addition the last two terms of c_{44} are replaced by $B\phi_o/(16\pi^2\tilde{\lambda}_c^2)$. These replacements guarantee that the elastic moduli vanish at H_{c2}. For YBCO the temperature dependence of the penetration depths and coherence lengths are given by $\lambda(T) = \lambda(0)(1 - (T/T_c))^{-1/3}$ [23] and $\xi_{ab}(T) = \xi_{ab}(0)(1 - (T/T_c))^{-1/2}$, respectively. For BSCCO whose premelting field is two orders of magnitude below H_{c2}, $\lambda^2(T) = \lambda^2(0)/(1 - (T/T_c)^4)$ and $\xi_{ab}^2(T) = \xi_{ab}^2(0)/(1 - (T/T_c)^4)$ [20].

The free energy density f_w due to the energy cost of adding a vacancy or interstitial vortex line is difficult to calculate accurately [10]. However, we can write down a plausible form for f_w by noting that a straight line defect parallel to the c-axis produces both shear and bulk (but not tilt) distortions of the vortex lattice. For example, if a defect at the origin produces a displacement

u that satisfies $\nabla \cdot \mathbf{u} = v_o \delta(\mathbf{r})/s$ where $\delta(\mathbf{r})$ is a two dimensional delta function, then $u_\alpha(\mathbf{k}) = i k_\alpha/k^2$ [10]. Inserting this in (4), we find that $f_w = (c_{66} + \overline{c}_B)/2$ where $\overline{c}_B = \sum_{\mathbf{k}} c_B(q=0, \mathbf{k})$. Generalizing this to allow for a more complicated distortion and for a concentration n of line defects, we write [14]

$$f_w = \int_0^n dn(\alpha_1 c_{66} + \alpha_2 \overline{c}_B) \qquad (6)$$

where α_1 and α_2 are dimensionless constants. We expect the isotropic distortion to be small, i.e., $\alpha_2 \ll 1$, and the shear deformation to dominate, i.e., $\alpha_1 \gg \alpha_2$. Integrating over n allows the elastic moduli to depend on defect concentration. We will assume that c_B is independent of n since we believe that the bulk modulus of the vortex solid is roughly the same as that of the soft solid phase. To find $c_{66}(n)$ [14], we use its definition $c_{66} = \partial^2 f/\partial \varepsilon^2$ where ε is the shear strain. Assuming that c_B has negligible shear strain dependence, we find $c_{66}(n) = c_{66}(0) + \alpha_1 \int_0^n (\partial^2 c_{66}(n)/\partial \varepsilon^2) dn$ or

$$\frac{\partial c_{66}(n)}{\partial n} = \alpha_1 \frac{\partial^2 c_{66}(n)}{\partial \varepsilon^2} \qquad (7)$$

If we shear the lattice in the ab plane along rows separated by a distance d, the shear modulus must be periodic in displacements equal to the lattice constant a_o. We describe this with the simplest even periodic function: $c_{66}(u) = c_{66}(u=0)\cos(2\pi u/a_o) = c_{66}(\varepsilon=0)\cos(2\pi d\varepsilon/a_o)$ where $\varepsilon = u/d$. Then $\partial^2 c_{66}(n)/\partial \varepsilon^2 = -\beta c_{66}(n)$, where $\beta = 4\pi^2 d^2/a_o^2$. Combining this with (7), we obtain $c_{66}(n) = c_{66}(0)\exp(-\alpha_1 \beta n)$. Thus the shear modulus softens exponentially with the defect concentration n. This softening lowers the energy cost to introduce further defects, and increases the vibrational free energy f_{vib} when $c_{66}(n)$ is used in a_{ij}. Substituting $c_{66}(n)$ into our expression (6) for f_w yields

$$f_w = \frac{c_{66}(n=0)}{\beta}(1 - e^{-\alpha_1 \beta n}) + \alpha_2 \overline{c}_B n \qquad (8)$$

The last term we need to consider is f_{wan}, the free energy due to the wandering of the defect lines over distances large compared to the lattice spacing. We can estimate f_{wan} with the following expression [10]

$$f_{wan} \approx -\frac{k_B T}{\ell_z a_o^2} \ln(m_\ell) \qquad (9)$$

where $m_\ell = 3$ for a triangular lattice (BSCCO) and $m_\ell = 4$ for a square lattice (YBCO). ℓ_z can be thought of as the distance along the z–axis that it takes for the defect line to wander a transverse distance of one lattice spacing a_o. To go from one vacancy or interstitial site to the next, the defect line segment must jump over the barrier between the two positions. This gives ℓ_z a thermally activated form: $\ell_z \sim \ell_o \exp(-E/k_B T)$, where

$\ell_o \approx a_o(\epsilon_1/\epsilon_B)^{1/2}$ and $E \approx a_o(\epsilon_1 \epsilon_B)^{1/2}$. ϵ_1 is the line tension and is given by $\epsilon_1 \sim (\epsilon_o/\gamma^2)\ln(a_o/\xi_{ab})$. Numerical simulations [10] indicate that the barrier height ϵ_B is small and we use $\epsilon_B = 2.5 \cdot 10^{-3}\epsilon_o$. f_{wan} itself is quite small compared to the other terms because of the high energy cost of vortex displacements. For example, in the soft solid phase at the transition f_{wan} is about two orders of magnitude smaller than f_w or f_{vib}. Thus the transition is not driven by a proliferation of wandering defect lines because near the transition the high energy cost of vortex displacements is not sufficiently offset by the entropy of the meandering line [10].

Before we plot f versus n, we note that the difference between B and H is negligible for YBCO but can be a significant fraction of the premelting field H_p for BSCCO. To find the value of B to use in the Helmholtz free energy density f, we minimize the Gibbs free energy density G, i.e., $\partial G/\partial B = 0$ where $G = f - \mathbf{B} \cdot \mathbf{H}/4\pi$. Since the concentration dependence of B is negligible, we find B for $n = 0$ for each value of H and T. Typical plots of $\Delta f = f(n) - f(0) = f_w + \Delta f_{vib}$ versus n are shown in the inset of figure 1. The double well structure of Δf is characteristic of a first order phase transition. The equilibrium transition occurs when both minima have the same value of Δf. We associate the minimum at $n = 0$ with the vortex solid and the minimum at finite n with a soft vortex solid that has a small but finite shear modulus. The defect concentration at the transition is only a few percent. At higher concentrations Δf increases with increasing n because introducing defects costs compressional energy which is proportional to the bulk modulus. Thus defects do not proliferate. As an estimate of the softness at the transition, for $n = 5\%$, $c_{66}(n) \sim 0.2 c_{66}(0)$ for BSCCO. The strain field $\varepsilon_{\alpha\beta}^d(k)$ produced by the defect determines whether the shear modulus is zero in the high temperature phase [24]. For dislocation loops, $\varepsilon_{\alpha\beta}^d(k)$ is singular as $k \to 0$, and the shear modulus is zero at $k = 0$ [24]. For vacancy and interstitial lines $\varepsilon_{\alpha\beta}^d(k)$ is finite, and hence the shear modulus is nonzero.

In Figure 1 we fit the experimental first order transition curves in the $H - T$ plane using 2 adustable parameters: α_1 and α_2. As expected, $\alpha_1 \gg \alpha_2$ and $\alpha_2 \ll 1$ (see Figure 1). The geometrical quantity β can have several values for a given lattice structure, depending on which planes are sheared. We choose $\beta = \pi^2 \tan^2 \phi$ where ϕ is the angle between primitive vectors. Decoration experiments on BSCCO find a triangular lattice [17], so we use $\phi = 60^o$. For YBCO we choose $\phi = 44.1^o$ which is very close to a square lattice which has $\phi = 45^o$. Maki [25] has argued that the d-wave symmetry of the order parameter yields a square vortex lattice tilted by 45° from the $a-$axis. Experiments [26–28] on YBCO find ϕ ranging from 36° to 45°.

We can calculate the jump in magnetization ΔM at the transition using $\Delta M = -\partial \Delta G/\partial H|_{T=T_p}$. The jump

in entropy Δs is given by $\Delta s = -v_o \partial \Delta G / \partial T|_{H=H_p}$ where Δs is the entropy change per vortex per layer. The results are shown in Figure 2. We have checked that our results satisfy the Clausius-Clapeyron equation $\Delta s = -(v_o \Delta B / 4\pi) dH_p / dT$. We obtain good agreement with experiment well below T_c. Near T_c it is thought that the entropy jump is enhanced by microscopic degrees of freedom [29,30] which are not included in our model.

We can compare our results with the Lindemann criterion by calculating the mean square displacement $< |u|^2 >$ at the transition using eq. (3): $< |u|^2 >= -(2k_B T/v_o) \sum_{\alpha \mathbf{k} q} \partial \ln Z_{vib} / \partial A(\alpha \mathbf{k} q)$ where A is the diagonal matrix similar to a_{ij} and α labels the 2 eigenvalues. Defining the Lindemann ratio c_L by $c_L^2 =< |u|^2 > /a_o^2$, we find that $c_L \approx 0.25$ for YBCO at $H_p = 5$ T and that $c_L \approx 0.11$ for BSCCO at $H_p = 200$ G. Here we have used the same values of the parameters that were used to fit the phase transition curves in Figure 1. These values of c_L are consistent with previous values [1,2,31].

Experiments have found little, if any, hysteresis [3,7,9]. This is consistent with our calculations. We can bound the hysteresis by noting the range of temperatures between which the soft solid minimum appears and the solid minimum disappears. Typical values for the width of this temperature range are 300 mK for YBCO at $H = 5T$ and 1.3 K for BSCCO at $H = 200$ G. Another measure of the hysteresis can be found in the plots of Δf versus n. The barrier height V_B between the minima is low ($V_B v_o \sim 30$ mK) which is consistent with minimal hysteresis.

In going from the normal metallic phase to the vortex solid, two symmetries are broken: translational invariance and gauge symmetry which produces the superconducting phase coherence along the magnetic field. In the soft solid phase, longitudinal superconductivity is destroyed by the wandering of the defect lines which become entangled with the soft solid vortices. (A vortex solid with entangled vortex lines has been termed a supersolid [10,11].) Even though line wandering is energetically costly and therefore rare, it does occur. As a result, the correlation length along the c–axis will be quite long. This is consistent with measurements in YBCO of the c–axis resistivity which find that there is loss of vortex velocity correlations for samples thicker than 100 μm [32–34]. For samples thicker than the longitudinal correlation length, the loss of longitudinal superconductivity coincides with the premelting transition [35]. This agrees with experiments which indicate that the loss of superconducting phase coherence along the c–axis coincides with the first order transition [32–34].

Since the soft solid is a lattice with a few percent of defect lines, the Fourier transform of the density-density correlation function should exhibit Bragg peaks. Relative to the ordinary vortex solid, the intensity of these peaks would be slightly diminished by the defect lines, so it would be difficult to detect the transition via neutron scattering. In going from the soft solid to the normal metallic state, translational invariance is regained by a first order melting transition. Thus there are two transitions: the premelting transition and the melting of the soft solid. Melting is observable in small angle neutron scattering experiments [36] which see a rapid decrease in the intensity of the Bragg spots. The region of the phase diagram where the soft solid exists may be quite narrow, of order a degree or less in temperature [13]. There is the intriguing possibility that our scenario of two transitions may be related to the peak effect in which the critical current as a function of temperature or field is observed to sharply increase below the melting transition [13]. This increase is believed to result from the enhanced pinning of flux lines due to the softening of the shear modulus c_{66} [37].

To summarize we have discussed the possibility that a vortex lattice melts in two stages. First it undergoes a first order premelting transition into a soft solid followed by another first order phase transition into a liquid. The premelting transition is induced by vacancy and interstitial vortex lines that soften the shear modulus and enhance the vibrational entropy. The entanglement of these defect lines with the vortex lines of the soft solid leads to the loss of longitudinal superconducting phase coherence. However, the correlation length corresponding to longitudinal superconductivity is quite long because line wandering is energetically costly and therefore rare. We obtain good agreement with the experimentally measured curve of transition temperature versus field, latent heat, and jumps in magnetization for BSCCO and YBCO. The Lindemann ratio c_L is $\sim 11\%$ for BSCCO and $\sim 25\%$ for YBCO. The hysteresis is small.
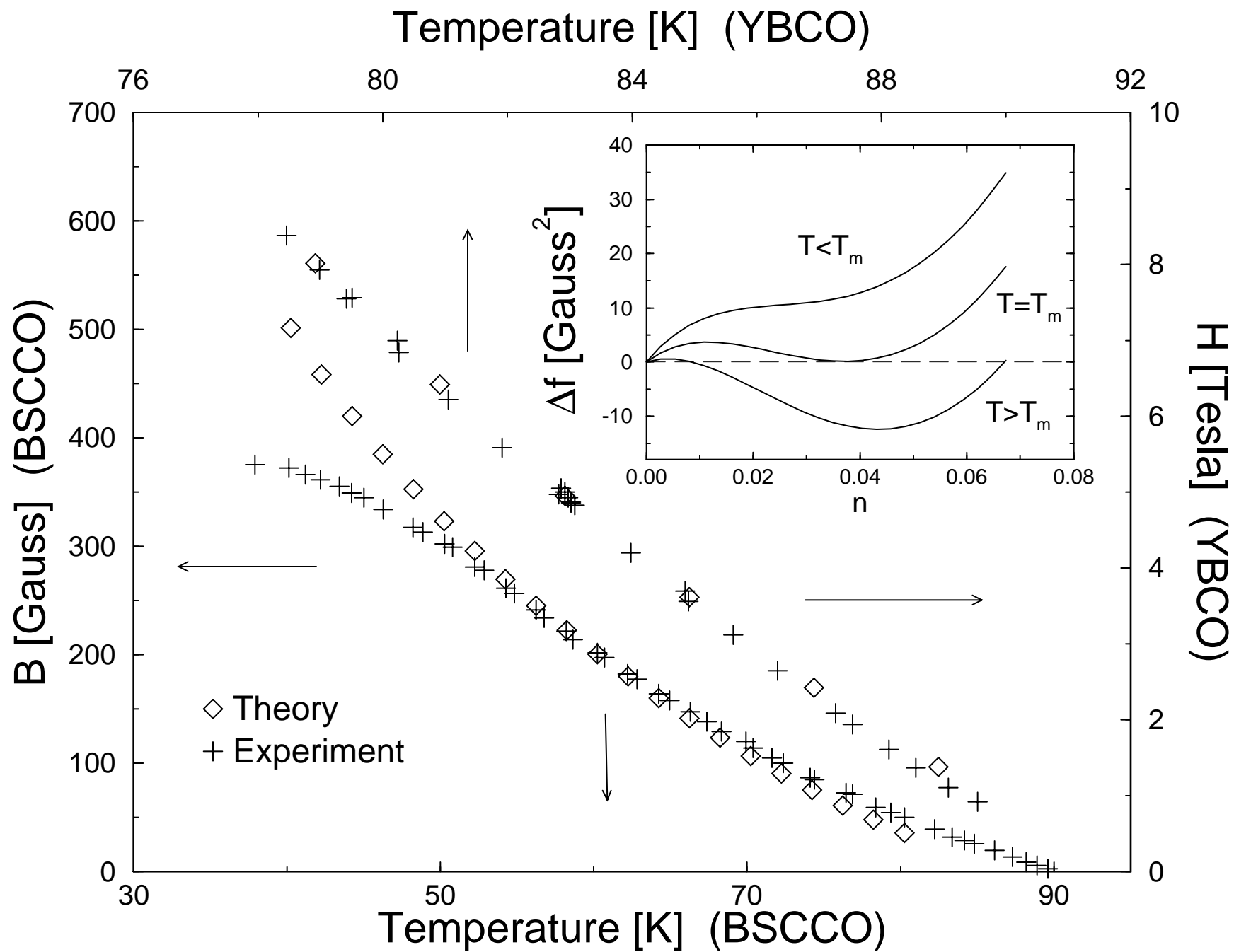
[1] G. Blatter *et al.*, Rev. Mod. Phys. **66**, 1125 (1994).

[2] E. H. Brandt, Rep. Prog. Phys. **58**, 1465 (1995).

[3] H. Safar *et al.*, Phys. Rev. Lett. **70**, 3800 (1993).

[4] R. Liang, D. A. Bonn, and W. N. Hardy, Phys. Rev. Lett. **76**, 835 (1996).

[5] U. Welp *et al.*, Phys. Rev. Lett. **76**, 4809 (1996).

[6] A. Schilling *et al.*, Nature **382**, 791 (1996).

[7] E. Zeldov *et al.*, Nature **375**, 373 (1995).

[8] D. T. Fuchs *et al.*, Phys. Rev. B **54**, R796 (1996).

[9] C. D. Keener *et al.*, Phys. Rev. Lett. **78**, 1118 (1997).

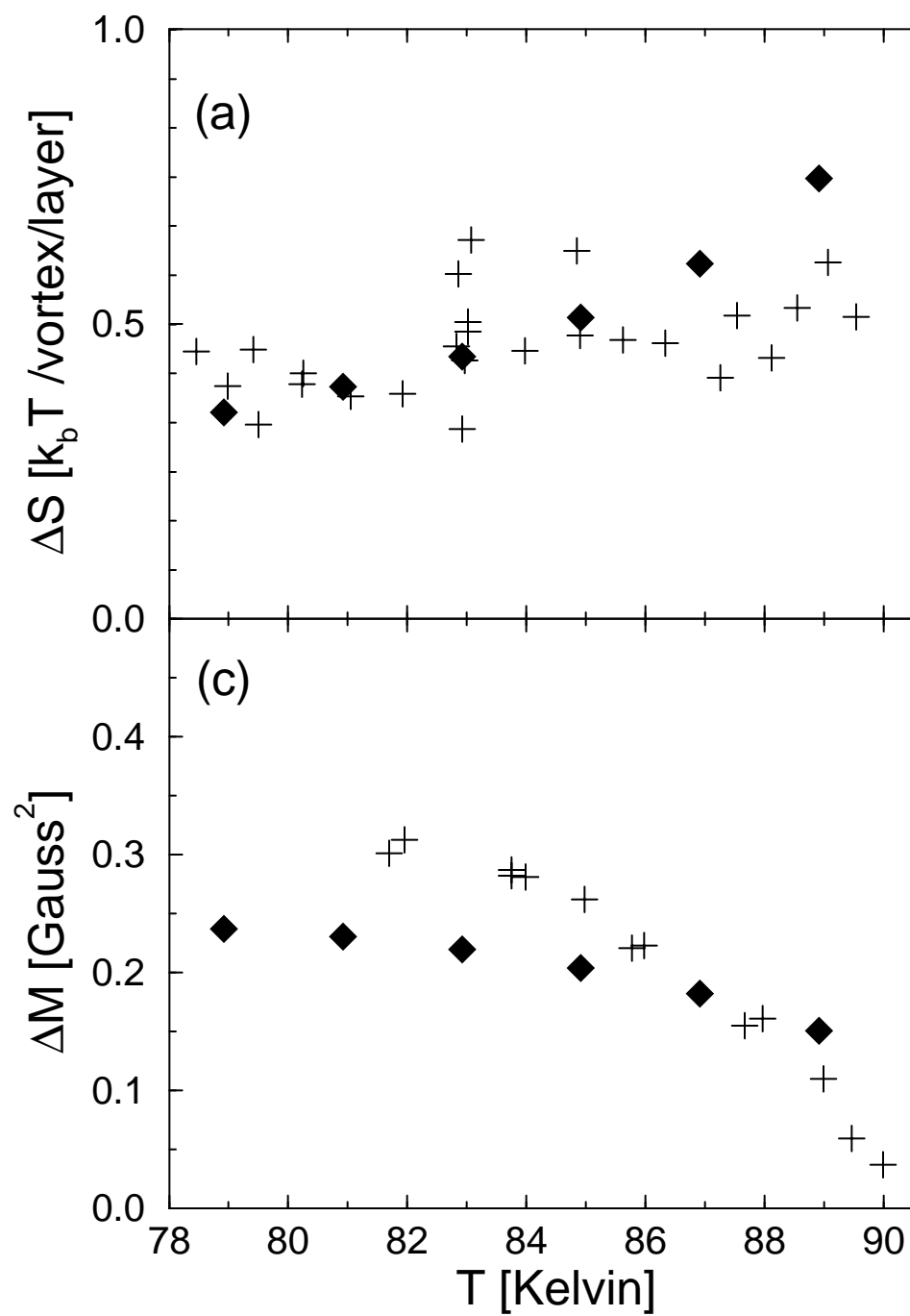[10] E. Frey, D. R. Nelson, and D. S. Fisher, Phys. Rev. B **49**, 9723 (1994).

[11] D. R. Nelson, in *Phenomenology and Applications of High-Temperature Superconductors*, edited by K. Bedell *et al.* (Addison-Wesley, New York, 1991), pp. 187–242.

[12] W. K. Kwok *et al.*, Phys. Rev. Lett. **76**, 4596 (1996).

[13] W. K. Kwok, J. A. Fendrich, C. J. van der Beek, and G. W. Crabtree, Phys. Rev. Lett. **73**, 2614 (1994).

[14] A. V. Granato, Phys. Rev. Lett. **68**, 974 (1992).

[15] F. P. Preparata and M. I. Shamos, *Computational Geometry* (Spinger-Verlag, New York, 1985).

[16] S. Ryu and D. Stroud, Phys. Rev. B **54**, 1320 (1996).

[17] P. Kim, Z. Yao, and C. M. Lieber, Phys. Rev. Lett. **77**, 5118 (1996).

[18] H. Pastoriza and P. H. Kes, Phys. Rev. Lett. **75**, 3525 (1995).

[19] H. Wu, N. P. Ong, R. Gagnon, and L. Taillefer, Phys. Rev. Lett. **78**, 334 (1997).

[20] M. Tinkham, *Introduction to Superconductivity*, 2nd ed. (McGraw-Hill, New York, 1996).

[21] P. G. de Gennes, *Superconductivity of Metals and Alloys* (Addison-Wesley, Redwood City, 1989).

[22] L. N. Bulaevskii, M. Ledvij, and V. G. Kogan, Phys. Rev. Lett. **68**, 3773 (1992).

[23] S. Kamal *et al.*, Phys. Rev. Lett. **73**, 1845 (1994).

[24] M. C. Marchetti and D. R. Nelson, Phys. Rev. B **41**, 1910 (1990).

[25] H. Won and K. Maki, Phys. Rev. B **53**, 5927 (1996).

[26] M. Yethiraj *et al.*, Phys. Rev. Lett. **70**, 857 (1993).

[27] B. Keimer *et al.*, Phys. Rev. Lett. **73**, 3459 (1994).

[28] I. Maggio-Aprile *et al.*, Phys. Rev. Lett. **75**, 2754 (1995), our ϕ equals half the angle cited in the experiments.

[29] M. J. W. Dodgson, V. B. Geshkenbein, H. Nordborg, and G. Blatter, condensed matter preprint number 9705220 (unpublished).

[30] A. I. M. Rae, E. M. Forgan, and R. A. Doyle, condensed matter preprint number 9706108 (unpublished).

[31] A. Houghton, R. A. Pelcovits, and A. Sudbo, Phys. Rev. B **40**, 6763 (1989).

[32] D. Lopez, E. F. Righi, G. Nieva, and F. de la Cruz, Phys. Rev. Lett. **76**, 4034 (1996).

[33] D. Lopez *et al.*, Phys. Rev. B **53**, R8895 (1996).

[34] D. Lopez, 1996, private communication.

[35] T. Chen and S. Teitel, Phys. Rev. Lett. **74**, 2792 (1995).

[36] R. Cubitt *et al.*, Nature **365**, 407 (1993).

[37] A. I. Larkin, M. C. Marchetti, and V. M. Vinokur, Phys. Rev. Lett. **75**, 2992 (1995).

FIG. 1. First order phase transition curves of magnetic field versus temperature. for YBCO and BSCCO. Parameters used for YBCO are $\alpha_1 = 2.55$, $\alpha_2 = 0.01485$, $\phi = 44.1^o$, $\lambda_{ab}(0) = 1186\mathring{A}$ [23], $s = 12\mathring{A}$, $\xi_{ab}(0) = 15\mathring{A}$, $\gamma = 5$, and $T_C = 92.74$ K. Parameters used for BSCCO are $\alpha_1 = 1.0$, $\alpha_2 = 0.00705$, $\phi = 60^o$, $\lambda_{ab}(0) = 2000\mathring{A}$, $s = 14\mathring{A}$, $\xi_{ab}(0) = 30\mathring{A}$, $\gamma = 200$, and $T_C = 90$ K. For BSCCO we use the low field form of the elastic moduli from (5) and for YBCO we use the high field form. For f_o we use (1) for BSCCO and (2) for YBCO. (For BSCCO we plot B vs. T because that is what ref. [7] measured.) The experimental points for YBCO come from ref. [6] and those for BSCCO come from ref. [7]. Inset: Typical Δf versus n.

FIG. 2. (a) and (b): Entropy jump Δs per vortex per layer versus T_p at the transition for YBCO and BSCCO. The experimental points for YBCO are from [6] and those for BSCCO are from [7]. (c) and (d): Magnetization jump ΔM versus T_p at the first order phase transition for YBCO and BSCCO. The experimental points for YBCO are from [5] and those for BSCCO are from [7]. For the theoretical points the values of the parameters are the same as in Figure 1 for all the curves.